Dalton Transactions

Luminescent Pt(2,6-bis(N-methylbenzimidazol-2-yl)pyridine)X^+: A comparison with the spectroscopic and electrochemical properties of Pt(tpy)X^+ (X = Cl, CCPh, Ph, or CH_3)

Journal:	*Dalton Transactions*
Manuscript ID	DT-ART-04-2020-001496.R1
Article Type:	Paper
Date Submitted by the Author:	19-Jun-2020
Complete List of Authors:	Shingade, Vikas; University of Cincinnati, Chemistry Grove, Levi; University of Cincinnati, Chemistry

ARTICLE

Luminescent Pt(2,6-bis(*N*-methylbenzimidazol-2-yl)pyridine)X^+: A comparison with the spectroscopic and electrochemical properties of Pt(tpy)X^+ (X = Cl, CCPh, Ph, or CH_3)†

Received 00th April 20xx,
Accepted 00th April 20xx

DOI: 10.1039/x0xx00000x

Vikas M. Shingade,*[a] Levi J. Grove [a] and William B. Connick‡[a]

A series of platinum(II) pincer complexes of the formula Pt(mbzimpy)X^+, **1**(a-d), (mbzimpy = 2,6-bis(N-methylbenzimidazol-2-yl)pyridine; X = Cl; (**a**), CCPh; (**b**), Ph; (**c**), or CH_3; (**d**), CCPh = phenylacetylide, and Ph = Phenyl) have been synthesized and characterized. Electronic absorption and emission, as well as electrochemical properties of these compounds, have been investigated. Pt(tpy)X^+ analogs (tpy = 2,2′;6′2′′-terpyridine), **2**(a-d), have also been investigated and compared. Electrochemistry shows that **1** and **2** analogs undergo two chemically reversible one-electron reduction processes that are shifted cathodically along the a < b < c < d series. Notably, these reductions occur at slightly higher negative potentials in the case of **1**. The absorption spectra of **1** and **2** in acetonitrile exhibit ligand-centered (^{1}LC) transitions ($\varepsilon \approx 10^4$ M^{-1} cm^{-1}) in the UV region and metal-to-ligand-charge transfer (^{1}MLCT) transitions ($\varepsilon \approx 10^3$ M^{-1} cm^{-1}) in the visible region. The corresponding visible bands of **1b** and **2b** have been assigned to ^{1}(LLCT/MLCT) mixed state (LLCT: ligand-to-ligand-charge transfer). The preceding ^{1}LC and ^{1}MLCT transitions of **1** occur at lower energies than that of **2**. These ^{1}LC transitions have distinctly been blue-shifted along a < c < d in **2**, but occur at nearly identical energies in **1**. Conversely, ^{1}MLCT transitions are red-shifted along a < c < d in both the analogs. The 77 K glassy solutions of **1** and **2** exhibit intense vibronically-structured emission band at λ_{max}(0-0) in the 470-560 nm range. This band is red-shifted along b < a ≤ c < d in **1** and along a ≤ d ≈ c << b in **2**. The main character of these emissions is assigned to ^{3}LLCT emissive state in **1b** and **2b**, whereas to ^{3}LC in the rest of the compounds. Relative stabilization of these spin-forbidden emissive states is discussed by invoking configuration mixing with the higher-lying ^{3}MLCT state.

Introduction

Square-planar platinum(II) complexes with 2,2';6',2''-terpyridine[1-15] and 2,6-bis(N-alkylbenzimidazol-2-yl)pyridine[16-24] pincer ligands have attracted widespread interest because of their intriguing spectroscopic properties as well as their potential utility in applications ranging from chemical sensing to biomolecular interactions, including DNA intercalation and b-iological labelling, to catalysis.[25-31] For example, simple solid salts (*cf.* double salts[32-35]) of **1a** are vapochromic, undergoing a distinct color change and change in luminescence properties upon exposure to different volatile organic compounds (VOCs).[16, 17, 36, 37] Grove *et al*.[16] have proposed that the sorption of certain VOCs causes a decrease in Pt..Pt contacts, resulting in dramatic changes in colors and spectroscopic properties of these compounds. It is widely accepted that the luminescence from stacked platinum(II) polypyridyl complexes with short Pt..Pt contacts (< 3.5 Å) typically originates from a lowest mixed-metal-to-ligand charge-transfer (MMLCT) state, involving an unoccupied π* level of the aromatic heterocyclic ligand and a filled dσ* orbital, which derives primarily from the interaction of the dz^2 orbitals of adjacent Pt atoms (Figure S1 ESI†). Interestingly, simple solid salts of **2a** exhibit different colorimetric responses to VOCs than their **1a** counterparts.[38, 39] These differences are surely related to the shapes, steric properties, and intermolecular interactions of the molecules, as well as differences in the electronic properties of **1a** and **2a**.

Previous studies provide some insight into the potential complexities of the less-studied Pt(mbzimpy)X^+ system. For example, Hill *et al*.[1, 2] have noted that the electronic structure of Pt(tpy) is perturbed by ancillary ligands and/or the surrounding medium. Hill *et al*. further noted that the low-lying π* orbital (LUMO) in Pt(tpy) unit is significantly stabilized compared to $Ru(tpy)_2^{2+}$ complex. The origin of this effect was attributed to mixing of the π*(tpy) orbital with the unoccupied $6p_z$(Pt) orbital, and an analogous effect involving a π*(mbzimpy) orbital is anticipated for **1a**. On the other hand, Che and others[3, 40-45] have shown that the spin-allowed tpy ligand-centered absorption profile of Pt(tpy)L^{n+} varies with the ancillary ligand (L: Cl, Br, I, SCN, or N_3, n = 1; and NH_3, n = 2) in a manner suggestive of significant configuration interaction involving the low-lying, spin-allowed ligand-centered (^{1}LC) and metal-to-ligand charge-transfer (^{1}MLCT) states. Therefore, orbital mixing may play an important role in the spectroscopy of related mbzimpy complexes. A comparison of pKa values[46] of

[a] *Department of Chemistry, University of Cincinnati, P.O. Box 210172, Cincinnati, OH 45221-0172*

‡ Professor William B. Connick passed away in 2018.

†Electronic Supplementary Information (ESI) available: [Synthesis and characterization, NMR, absorption, excitation, and emission spectra, cyclic voltammograms, and table of absorption maxima of platinum(II) and related compounds are provided in PDF format]. See DOI: 10.1039/x0xx00000x

benzimidazoles and pyridine suggests that mbzimpy has a stronger σ-donor capacity than tpy. On the other hand, a comparison of the X-ray structures of the known transition metal mbzimpy[37, 47-50], and tpy[9, 51-56] complexes shows that mbzimpy has N-M-N bite angles that are 2-4° smaller than that of the tpy, as expected for the geometric constraints of the five-membered imidazole group. Notably, the redox chemistry of ruthenium mbzimpy and tpy complexes affords some insight into the ligand donor properties. For example, Haga[57] and others[58-60] show that the oxidation of ruthenium from +2 to +3 in $Ru(mbzimpy)_2^{2+}$ (+0.86 V vs. Ag/AgCl) is shifted cathodically by ~ 0.5 V from that of the $Ru(tpy)_2^{2+}$ (+1.31 V vs. Ag/AgCl). This result is consistent with the notion that mbzimpy is a stronger electron donor. Provided that, it is unclear how the similar effect compares in platinum(II) complexes with mbzimpy and tpy ligands.

To better understand the influence of the mbzimpy and tpy ligands, as well as the influence of the ancillary ligand, on a platinum(II) center, herein, we have undertaken experimental investigation of the electronic structures of a series of $Pt(mbzimpy)X^+$ and $Pt(tpy)X^+$ complexes in Scheme 1. Notably, we anticipate that σ-donation by the ancillary ligand will increase along the Cl < CCPh < Ph < CH_3 series, whereas π-donation should be increased along the Ph, CCPh < CH_3 << Cl series.

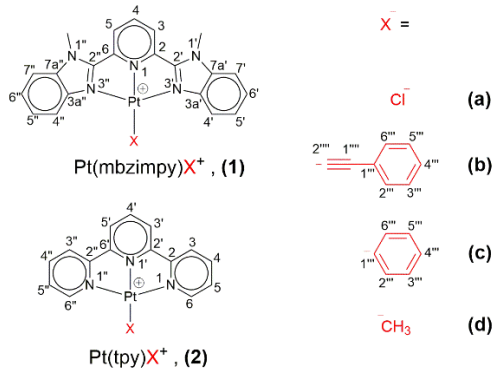

Scheme 1. Schematic representation and atom numbering for the compounds in this study. $(PF_6)^-$ is the anion.

Experimental Section

Materials and Methods. Compounds in scheme 1 were synthesized in analytically pure form following the modifications of the published procedures for **2(a-d)**. [4, 61-65] Details of the syntheses are provided in the supplementary information. Characterization data of **1(a-b)** are summarized below. For spectroscopic and electrochemical characterization, high purity anhydrous dimethylformamide (DMF) and acetonitrile were obtained from Burdick and Jackson, whereas butyronitrile, ethanol, and methanol were obtained from Sigma-Aldrich. Tetrabutylammonium hexafluorophosphate (TBAH) supporting electrolyte was obtained from Sigma-Aldrich. For emission and excitation studies, ethanol: methanol: DMF (10:10:1 v/v) solvent mixture (abbreviated as EMD) was used. Deuterated solvents were purchased from Cambridge Isotope Laboratories. The 1D (^1H, ^{13}C, and ^{195}Pt) and in several instances 2D (COSY, HSQC, and/or NOE) NMR spectra were recorded at room temperature (20-25 °C). In the case of **1b**, a series of ^1H NMR spectra were also recorded over the temperature range of 25-70 °C. 2D NOE experiments were run with mixing time, τ_m, of 75 ms. Spectra are reported in parts per millions (ppm) relative to TMS (δ = 0 ppm), or the residual internal standard (~ the protic solvent impurity) [$(CD_3)_2SO$, δ_H = 2.50 ppm; and δ_C = 39.52 ppm for CD_3SOCD_2H], or relative to a saturated solution of $Na_2[PtCl_6]$ in D_2O in the case of ^{195}Pt NMR. Elemental analyses were performed by Atlantic Microlab, Norcross, GA.

Instrumentation. The ^1H, ^{13}C, COSY, and HSQC NMR spectra were recorded using Bruker AC 400 MHz instrument, whereas NOE and ^{195}Pt NMR spectra were recorded using a Bruker DMX 500 MHz and a Bruker AMX 400 MHz instruments, respectively. Mass spectra were obtained by electrospray ionization using either an Ionspec HiRes ESI-FTICRMS instrument or a Micromass Q-TOF-II instrument. The observed isotope patterns agreed well with those predicted based on natural isotopic abundances (only monoisotopic masses are provided here). Infrared spectra were collected using a Nicolet 6700 FTIR spectrometer. UV-visible absorption spectra were recorded using an HP8453 diode array spectrometer on samples contained in 1 cm and/or 1 mm pathlength quartz cuvettes. Cyclic voltammetry (CV) measurements were performed at room temperature using a BAS100b potentiostat (Bioanalytical Systems) and a standard three-electrode cell consisting of either a 2.11 mm^2 platinum disk or a 7.07 mm^2 glassy carbon disk working electrode; as specified, Ag/AgCl (containing 3.0 M NaCl aqueous solution) reference electrode, and a platinum wire auxiliary electrode. Scans were recorded of ~1 mM DMF solutions containing 0.1 M TBAH which was recrystallized at least twice from methanol and dried under vacuum before use. Between scans, the working electrode was polished with 0.05 mm alumina, rinsed with distilled water and wiped dry using a Kimwipe. Reported potentials are referenced versus Ag/AgCl (3.0 M NaCl) and are not corrected for junction potential. Peak currents (i_p) were estimated with respect to the extrapolated baseline current, as described by Kissinger and Heineman.[66] The values of $(E_{pc}+E_{pa})/2$, which is an approximation of the formal potential of a redox couple, are referred to as $E°'$. Under these conditions, the ferrocene/ferrocenium couple occurs at 0.54 V, ΔE_p = 80 mV.

For emission and excitation studies, the 77 K glassy solution was prepared by inserting a quartz EPR tube containing the solution into a quartz-tipped finger dewar filled with liquid nitrogen. The data were collected using a SPEX Fluorolog-3 fluorimeter equipped with a double emission monochromator

and a single excitation monochromator. The emitted light was collected at 90° using an appropriate emission cutoff filter. The spectra were corrected for an instrumental response.

Characterization of **1a:** Yield: 85-90 %. MS-ESI (m/z): 570.08 $(PtC_{21}H_{17}N_5Cl)^+$, Calcd. 569.93. Anal. Calcd. for $C_{21}H_{17}N_5F_6ClPPt$: C, 35.28; H, 2.40; N, 9.80 %. Found: C, 34.98; H, 2.29; N, 9.63 %. ^{1}H NMR (400 MHz, 23.2 mM in $(CD_3)_2SO$, δ/ppm) δ_H 8.44 (1H, t, ^3J = 8.0 Hz, H_4), 8.25 (2H, d, ^3J = 8.0 Hz, H_3 and H_5), 7.34 (2H, d, ^3J = 8.0 Hz, $H_{4'}$ and $H_{4''}$), 7.22 (2H, dd, ^3J = 8.0 Hz, $H_{5'}$ and $H_{5''}$), 7.11 (2H, dd, ^3J = 8.0 Hz, $H_{6'}$ and $H_{6''}$), 6.85 (2H, d, ^3J = 8.0 Hz, $H_{7'}$ and $H_{7''}$), 3.74 (6H, s, N-CH_3). ^{13}C NMR (400 MHz, 23.2 mM in $(CD_3)_2SO$, δ/ppm) δ_c 152.4, 147.0, 142.3 (C_4), 137.6, 133.3, 126.2 ($C_{5'}$ and $C_{5''}$), 125.5 ($C_{6'}$ and $C_{6''}$), 124.7 (C_3 and C_5), 114.8 ($C_{4'}$ and $C_{4''}$), 112.0 ($C_{7'}$ and $C_{7''}$), 32.17 (N-CH_3). ^{195}Pt NMR (26.2 mM, $(CD_3)_2SO$, δ/ppm) δ -2596.

1b: Yield: 70-75 %. MS-ESI (m/z): 635.15 $(C_{29}H_{22}N_5Pt)^+$, Calcd. 635.15. FT-IR, $\nu_{(C\equiv C)}$ = 2112 cm^{-1}. ^{1}H NMR (400 MHz, 46 μM in $(CD_3)_2SO$, 60 °C, δ/ppm) δ_H 8.67 (2H, d, J = 8 Hz, $H_{4'}$ and $H_{4''}$), 8.63 (2H, d, J = 8 Hz, H_3 and H_5), 8.58 (1H, t, J = 8 Hz, H_4), 8.02 (2H, d, J = 8 Hz, $H_{7'}$ and $H_{7''}$), 7.66 (4H, dd, J = 5.4 Hz, $H_{5'}$, $H_{5''}$, $H_{6'}$, and $H_{6''}$), 7.55 (2H, d, J = 7.6 Hz, $H_{2'''}$ and $H_{6'''}$), 7.46 (2H, dd, J = 7.4 Hz, $H_{3'''}$ and $H_{5'''}$), 7.33 (1H, t, J = 7.2 Hz, $H_{4'''}$), 4.48 (6H, s, N-CH_3). ^{13}C NMR (400 MHz, 54.6 mM in $(CD_3)_2SO$, δ/ppm) δ_c 155.6; 151.9; 146.6; 145.8 ((C_2, C_6), ($C_{2'}$, $C_{2''}$), ($C_{7a'}$, $C_{7a''}$), and ($C_{3a'}$, $C_{3a''}$)), 141.9 (C_4), 137.2; 132.9; 126.03 ($C_{1'''}$, $C_{1''''}$, and $C_{2''''}$), 130.9, 128.9, 125.8, 125.3, 124.2, 115.3, 114.4, 111.59 ($C_{4'''}$), 31.94 (N-CH_3). ^{195}Pt NMR (400 MHz, $(CD_3)_2SO$, δ/ppm) δ -3367.5

1c: Yield: 75-80 %. MS-ESI (m/z): 611.16 $(PtC_{27}H_{22}N_5)^+$, Calcd. 611.15. Anal. Calcd. for $C_{27}H_{22}F_6N_5PPt$: C, 42.87; H, 2.93; N, 9.26 %. Found: C, 42.62; H, 2.93; N, 9.23 %. ^{1}H NMR (400 MHz, 2.1 mM in $(CD_3)_2SO$, δ/ppm) δ_H 8.67 (2H, d, J = 8.0 Hz, H_3 and H_5), 8.56 (1H, t, J = 8.0 Hz, H_4), 8.00 (2H, d, J = 8.4 Hz, $H_{7'}$ and $H_{7''}$), 7.70 (2H, d, J = 6.8 Hz, $H_{2'''}$ and $H_{6'''}$), 7.49 (2H, dd, J = 7.6 Hz, $H_{6'}$ and $H_{6''}$), 7.23 (2H, dd, J = 7.8 Hz, $H_{5'}$ and $H_{5''}$), 7.22 (2H, dd, J = 7.8 Hz, $H_{3'''}$ and $H_{5'''}$), 7.14 (1H, t, J = 7.2 Hz, $H_{4'''}$), 6.53 (2H, d, J = 8.4 Hz, $H_{4'}$ and $H_{4''}$), 4.46 (6H, s, N-CH_3). ^{13}C NMR (400 MHz, $(CD_3)_2SO$, δ/ppm) δ_c 155.0, 146.4, 142.0 (C_4), 138.9 ($C_{2'''}$ and $C_{6'''}$), 138.8, 136.5 ($C_{1'''}$), 135.0, 127.0 ($C_{3'''}$ and $C_{5'''}$), 125.8 ($C_{5'}$ and $C_{5''}$), 125.7 ($C_{6'}$ and $C_{6''}$), 124.6 (C_3 and C_5), 123.9 ($C_{4'''}$), 117.0 ($C_{7'}$ and $C_{7''}$), 32.84 (N-CH_3). ^{195}Pt NMR (400 MHz, 51.2 mM in $(CD_3)_2SO$, δ/ppm) δ -3390.4

1d: Yield: 80 %. MS-ESI (m/z): 549.14 $(PtC_{22}H_{20}N_5)^+$, Calcd. 549.14. Anal. Calcd. for $C_{22}H_{20}F_6N_5PPt$: C, 38.05; H, 2.9; N, 10.08 %. Found: C, 38.28; H, 2.9; N, 10.22 %. ^{1}H NMR (400 MHz, 0.67 mM in $(CD_3)_2SO$, δ/ppm) δ_H 8.59 (2H, d, ^3J = 7.8 Hz, H_3 and H_5), 8.52 (1H, t, ^3J = 7.8 Hz, H_4), 7.93 (4H, d, ^3J = 8.2 Hz, $H_{4'}$, $H_{4''}$, $H_{7'}$ and $H_{7''}$), 7.59 (4H, m, $H_{5'}$, $H_{5''}$, $H_{6'}$ and $H_{6''}$), 4.36 (6H, s, N-CH_3), 1.98 (3H, s, $^2J_{Pt\text{-}H}$ = 79.2 Hz, Pt-CH_3). ^{13}C NMR (400 MHz, 29.4 mM in $(CD_3)_2SO$, δ/ppm) δ_c 154.1, 144.6, 140.8 (C_4), 138.7, 134.0, 126.1; 125.3 ($C_{5'}$; $C_{5''}$, and $C_{6'}$; $C_{6''}$), 124.1 (C_3 and H_5), 115.4; 112.1 ($C_{4'}$; $C_{4''}$, and $C_{7'}$; $C_{7''}$), 32.3 (N-CH_3), -25.6 (Pt-CH_3). ^{195}Pt NMR (400 MHz, 48 mM, $(CD_3)_2SO$, δ/ppm) δ -3346.2

Results and Discussion

Synthesis and Characterization. The mbzimpy ligand was obtained in high yield and purity optimizing the synthetic procedure reported by Addison *et al.* (see ESI†).[67] Homologues of Pt(mbzimpy)X$^+$ in Scheme 1, **1(a-d)**, were synthesized following modifications of literature procedures for the terpyridine analogs, **2(a-d)**;[4, 61-65] our recommended routes are outlined in Scheme 1S (ESI†). On occasion, we will refer to **1(a-d)** and **2(a-d)** analogs simply as **1** and **2**, respectively. **1** and **2** form yellow to orange-red air-stable solids, and in most cases, these colors are depending on whether samples are wet or dry. For spectroscopic comparison, $[Zn(mbzimpy)_2](PF_6)_2$ (**3**) complex also was synthesized (see ESI†).[47, 68] The products were obtained in analytically pure form and characterized by elemental analysis, mass spectrometry, multinuclear (^{1}H, ^{13}C, and ^{195}Pt) NMR, and in a few instances with FTIR spectroscopy. NMR assignments were made according to the numbering in Scheme 1 and by employing a combination of two or more 2D NMR techniques such as COSY, NOESY, and HSQC, as required.

^{1}H NMR spectra of the compounds above exhibit expected patterns of resonances (Figures S6-S24 ESI†). Notably, these patterns, excepting for **1c**, **2c**, **3**, and free mbzimpy and tpy, are concentration and temperature-dependent, which is consistent with a tendency for these compounds to aggregate in solution.[5, 32, 44, 69, 70] For example, in the case of **1b**, ^{1}H NMR spectra recorded over the concentration range of 46 μM - 4.8 mM in DMSO-d_6 at 60 °C (Figure S12 ESI†) show that all proton resonances are shifting monotonically upfield and broadening with increasing concentration. The reverse effect was noted when the temperature was increased (Figure S11 ESI†). These observations are consistent with a dynamic equilibrium between monomer and an aggregate, most likely supported by non-covalent Pt..Pt and/or mbzimpy..mbzimpy stacking interactions.[5, 32, 44, 69-76] Interestingly, variations in the sensitivity of proton chemical shifts to concentration and temperature suggest that changes in shielding are dependent on the specific stacking geometry of the aggregate. While understanding the nature of these aggregates is an interesting problem, this study is beyond the scope of this article and will comprehensively be discussed in our forthcoming article.[77] The only thing we would like to point out in here is that the complexes with mbzimpy show greater tendencies for aggregation in solutions than their tpy counterparts (For example, **1b** >> **2b**; Figures S12 and S18 ESI†).

FTIR spectra were recorded on solid samples of **1b** and **2b** to gain insight into relative donor properties of the triimine ligands. Direct comparison of the $\nu_{(C\equiv C)}$ stretching frequencies to that of the free phenylacetylene is problematic because the latter is solvent sensitive (e.g., CCl_4, 2119 cm^{-1}; $CHCl_3$, 2109 cm^{-1}).[78, 79] Nevertheless, the $\nu_{(C\equiv C)}$ of **1b** (2112 cm^{-1}) is indubitably lower than that of **2b** (2125 cm^{-1}). Under the assumption that electrostatic effects[80] are similar in the two complexes, these

results are consistent with the notion that **1b** has greater π-electron density available for Pt-C≡C π-back bonding as might be expected for mbzimpy having weaker π-accepting properties than tpy.

Electrochemistry. To better understand the electronic structures of **1(a-d)** and **2(a-d)**, cyclic voltammograms (CVs) were recorded on samples dissolved in 0.1 M TBAH/DMF solution (Figures 1, and S2 (ESI†), and Table 1). The electrochemistry of **2a** and **2b** have previously been described by the Gray and Yam groups, respectively.[2, 65, 81]

1(a-d) and **2(a-d)** undergo two chemically reversible one-electron reduction processes in DMF. In the case of **1(a-d)**, the 1st reduction occurs in the -0.75 to -1.06 V range, depending on the ancillary ligand. For each complex, the potential is cathodically shifted by 0.1 V from that of the mainly ligand-centered one-electron reduction[2, 18, 63, 65, 81-83] of the corresponding terpyridyl compound, **2(a-d)**. The results are consistent with the conclusion that the LUMO of the **1(a-d)** series is only slightly destabilized with respect to that of the **2(a-d)**. Compounds **1(a-d)** undergo a second reduction process in the -1.40 to -1.75 V range, which is cathodically shifted by ~ 0.2 V from that of the corresponding reduction process in **2(a-d)** analogs. There is some disagreement about the nature of the second reduction (LUMO+1) of platinum(II) polypyridyl complexes which has been suggested to involve addition of an electron to either predominantly metal-centered[2, 84, 85] or ligand-centered orbital.[18, 65, 69, 86]

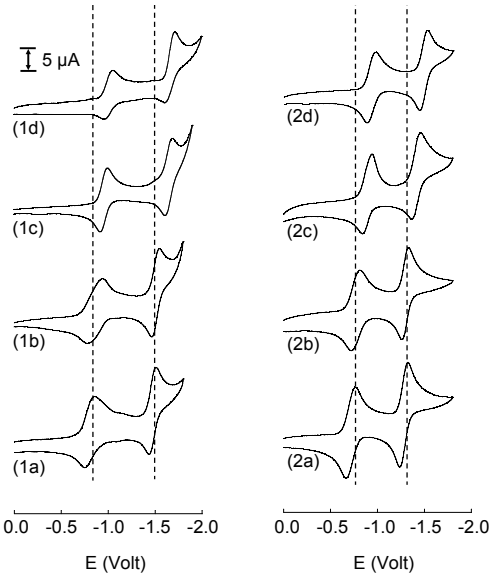

Figure 1. Cyclic voltammograms of **1** and **2** in 0.1 M TBAH/DMF at a scan rate of 100 mV/s. The working electrode was platinum, the auxiliary electrode was a platinum wire, and the reference electrode was Ag/AgCl in 3.0 M NaCl

For **1** and **2**, both reduction processes are slightly but monotonically shifted to negative potentials along the Cl < CCPh < Ph < CH_3 series of ancillary ligands, which suggests that electron donation by these ligands increases in the same order. Within the uncertainties of the estimated potentials, the correlation of the potentials of the mbzimpy and tpy series is excellent with essentially unitary slope.

Related late 1st, 2nd and 3rd-row transition metals with mbzimpy and tpy chelates display qualitatively similar reduction processes.[47, 57, 87] The reports by Haga[57] and others[58-60] show that ligand-centered reductions in $Ru(mbzimpy)_2^{2+}$ (-1.24, -1.55 vs. Ag/AgCl) and in $Ru(tpy)_2^{2+}$ (at -1.22, -1.46 V vs. Ag/AgCl) occur at essentially same potentials, which suggest that the ligand-centered low-lying π* orbitals (LUMO) in these complexes have virtually same energies. Notably, the metal-centered d^5/d^6-electron couple of $Ru(mbzimpy)_2^{3+/2+}$ (+0.86 V vs. Ag/AgCl) is shifted cathodically by ~ 0.5 V from that of $Ru(tpy)_2^{2+}$ (+1.31 V vs. Ag/AgCl), which is consistent with the notion that mbzimpy is a stronger electron donor than tpy. In comparison to these ruthenium and other related[47, 88] metal complexes, the first reduction wave of **1** and **2** has been substantially stabilized.[89] This effect in the case of **2a** has been suggested to have resulted from the coupling of the tpy π^* orbital with the higher lying empty $6p_z$(Pt) orbital.[2]

Table 1. Electrochemical potentials for **1** and **2** complexes[a], as determined by cyclic voltammetry.

Complexes	E_{pa}	$E°'_{+/0}$, (ΔE_p[c])	$E°'_{0/-}$, (ΔE_p[c])
1a		-0.80 (103)	-1.47 (76)
1b		-0.86(149)	-1.51 (72)
1c		-0.96 (75)	-1.65 (77)
1d		-1.01 (76)	-1.67 (100)
2a		-0.72(102)	-1.28 (86)
2b		-0.77 (88)	-1.30 (67)
2c		-0.89(102)	-1.42 (86)
2d		-0.93 (88)	-1.49 (79)
1b[d]	+1.30[b]	-0.86 (156)	-1.51 (78)
2b[d]	+1.31[b]	-0.77 (102)	-1.30 (78)
1c[d]	+1.54[b]	-0.96 (80)	-1.65 (102)
2c[d]	+1.57[b]	-0.89 (86)	-1.42 (90)

[a] $(PF_6)^-$ salts of platinum complexes in 0.1 M TBAH/DMF; Pt electrode; V vs. AgCl (3.0 M NaCl)/Ag. Couples are chemically reversible one-electron processes unless specified.

[b] Chemically irreversible under experimental conditions.

$E°' = (E_{pa} + E_{pc})/2$, (V); E_{pa} and E_{pc} are the anodic and cathodic peak potentials, respectively.

[c] The difference between the potentials of the forward (E_{pc}) and reverse (E_{pa}) peaks in mV.

[d] On a glassy carbon electrode.

In addition to the reductions processes (LUMO and LUMO+1) noted-above, **1b**, **1c**, **2b**, and **2c** also undergo chemically irreversible oxidation on a glassy carbon electrode within the experimental window (< +1.8 V) (Figure S2 ESI†). Based on the electrochemistry of related platinum compounds,[18, 63, 65, 81-83, 90-94] it seems probable that the oxidation process for **1c** and **2c** (at +1.54 for **1c** and +1.57 V for **2c**) is associated with metal oxidation, whereas oxidation of **1b**

and **2b** (at +1.30 V for **1b** and +1.31 V for **2b**) has a substantial contribution coming from the acetylene group. Although irreversible peak potentials cannot be considered as reliable estimates of redox potentials, it has not escaped our notice that the difference between the oxidation peak potential and the first reduction potential (2.16 eV for **1b** and 2.08 eV for **2b**) is remarkably similar to the HOMO-LUMO energy gap for **1b** and **2b**, that has previously been predicted by computational studies.[95]

Electronic Absorption Spectroscopy. The room-temperature absorption spectra of **1(a-d)** and **2(a-d)** in acetonitrile are presented in Figures 2 and S4 (ESI†). The absorption spectra of **3** and free triimine ligands[96, 97] are provided in Figure S3 (ESI†) for comparison.[47] Table S1 (ESI†) summarizes the absorption maxima of the aforementioned compounds in acetonitrile, dimethyl sulfoxide or solvent as specified. Data[3] for $Zn(tpy)_2^{2+}$ is also included for the comparison.

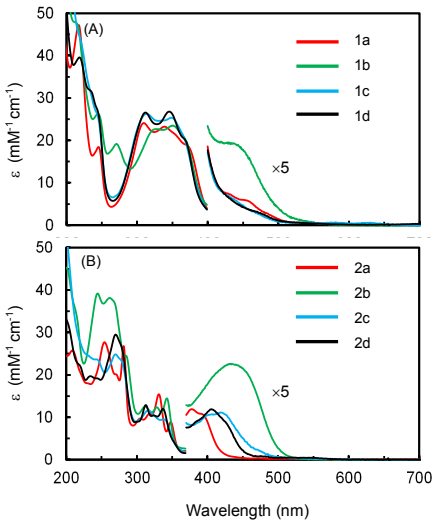

Figure 2. Electronic absorption spectra of 0.1 - 0.3 mM solutions of 1 (A) and 2 (B) in acetonitrile at room- temperature.

The absorption spectra of **1(a-d)** are characterized by a broad, intense, and weakly structured band originating in the 280-380 nm region with the molar absorptivity in the order of 10^4 M^{-1} cm^{-1} (Figure 2 A). The absorption spectra of **3** and free mbzimpy, although remain partially resolved, exhibit intense absorption band(s) in the same region, which suggests a presence of spin allowed, mbzimpy ligand-centered ^{1}LC transitions.[47, 88] Furthermore, vibronic spacings ranging from 1337-1504 cm^{-1} are diagnostic of $^1(\pi\rightarrow\pi^*)$ transitions.[47, 58]

Notably, the terpyridyl **2(a-d)** complexes exhibit two distinctly separate absorption bands in the 250-375 nm region (Figure 2 B), which are relatively more structured and occur at relatively higher energies.[3, 4, 65, 98] The first vibronically structured and moderately intense ($\varepsilon \approx 10^4$ M^{-1} cm^{-1}) band originating in 300-350 nm region is assigned to the low-lying $^1LC_1$ transitions, whereas the second band in 250-300 nm region with relatively high intensity is assigned to the next low-lying $^1LC_2$ transitions. Between **1** and **2** analogs, some of the spectral variations, such as intensity and bandwidth are comparable with those of the free ligands (Figure S3 ESI†). Interestingly, the $^1LC_1$ absorption band of **2(a-d)** is slightly, but distinctly, shifted to longer wavelengths along the $CH_3 \approx$ Ph < CCPh < Cl series of ancillary ligands.[3] Furthermore, the band profile (the shape and the vibronic intensities, including a number of vibronic peaks) of the LC transitions is varied with the ancillary ligand. In the case of **1(a-d)**, a comparable trend is not apparent because of having a poorly structured LC band, but the band shape is conspicuously varied with the changing ancillary ligand.

At the lower end of ^{1}LC transitions, each of the **2** exhibits relatively broad and weakly structured absorptions ($\varepsilon \approx 10^3$ M^{-1} cm^{-1}; 1200 -1400 cm^{-1} spacings) in the 360-450 nm range, which, excepting those from the **2b**, have been assigned to the metal-to-ligand-charge-transfer ^{1}MLCT [$d\pi(Pt) \rightarrow \pi^*(tpy)$] transitions.[3, 4, 65, 98] In the case of **2b**, these absorptions are relatively more intense and suggested to be originated from the ^{1}LLCT/^{1}MLCT mixed state [LLCT: ligand-to-ligand-charge transfer; $\pi(C\equiv C\text{-}Ph)\rightarrow\pi^*(tpy)$].[95] By analogy of **2** and related mbzimpy[16, 18, 37] complexes, the low energy (400-520 nm) absorption band of **1(a, c, d)** is assigned to ^{1}MLCT transitions. Similarly, the low energy band of **1b**, which shows a striking resemblance with that of the **2b**, is tentatively assigned to the ^{1}LLCT/^{1}MLCT mixed state. In comparison to **2**, the ^{1}MLCT bands of **1(a, c, d)** are weak and, adding further to our disadvantage, obscured by the extended tailing of the ^{1}LC bands and the poor spectroscopic resolution. As expected, the excitation measurements in the frozen EMD solutions countered the issue of low-resolution and yielded relatively well-resolved spectra, especially in the MLCT region (Figures 3 and S5 ESI†). These excitation measurements reveal structured features (1175-1550 cm^{-1} spacings) in the ^{1}MLCT region (which, however, look distinctly different from that of the **2**). Notably, the HOMO-LUMO transitions (at 457 nm) in analogous complex, [Pt(R,R′-bzimpy)Cl](PF_6) (R = $C_{12}H_{25}$, R′ = H), have been attributed to the LC (R,R′-bzimpy $\rightarrow$ R,R′-bzimpy) transitions by computational study.[18] At this point, our judgment of assigning the above-structured features to MLCT transitions comes purely from the perspective of intensities (relative molar absorptivities, ε) of the characteristically similar ^{1}MLCT and ^{1}LC bands in related platinum complexes. We also note that similar features are absent from the excitation spectrum of **3**. Excitation measurements further reveal that the ^{1}MLCT band of each of the **1** occurs at lower energies than that of the corresponding terpyridyl compound, **2**. For example, the ^{1}MLCT band of **1a** occurs at about ~3300 cm^{-1} lower in energy than that of the **2a**. Furthermore, we note that the ^{1}MLCT band of both **1** and **2** show a bathochromic shift (or stabilization) along the Cl < Ph < CH_3 series. Notably, in the case of **2**, the ^{1}MLCT band shifts along the Cl < Ph < CH_3 series are larger than that for the ^{1}LC

transitions. As noted earlier, a similar trend is not immediately apparent in the case of **1** because of having a poorly structured ^{1}LC band.

The effect of ancillary ligand donor properties on the energy and Frank-Condon factors of the $^1LC_1$ band of $Pt(tpy)L^{n+}$ complexes (L: Cl, Br, I, SCN, or N_3, n = 1; and NH_3, n = 2) has previously been documented by Che and co-workers.[40] This effect is attributed to the configuration interaction between $^1LC_1$ and ^{1}MLCT states.[40] In this model, ^{1}MLCT state undergoes stabilization (a shift to longer wavelengths) with an increasing σ donor capacity of an ancillary ligand, leading to widening of an energy gap between the low lying $^1LC_1$ and ^{1}MLCT states, as that, also noted for platinum(II) diimine complexes.[99, 100] This leads to the decreased mixing of the ^{1}LC and ^{1}MLCT states. As a result, the ^{1}LC band maximum is also expected to shift slightly to longer wavelengths. The energies of a ^{1}LC band of $Pt(tpy)L^{n+}$ including that of **2(a, c, d)**, however, do not model well with the two-state perturbation model, as used by Myrick, De Armond, and Blakely to describe mixing of ^{1}MLCT and $^1LC_1$ states in ruthenium(II) bipyridyl systems.[101] The spectra show unexplained variations in the $^1LC_1$ band maxima with stabilization of the MLCT states. For example, as noted above, the $^1LC_1$ state of **2(a, c, d)** is destabilized along the Cl < Ph < CH_3 series, while the ^{1}MLCT state along the same order is stabilized. We believe that sources of this complexity include contamination of spectra by solution aggregates,[45] π*(tpy)/6p_z(Pt) orbital mixing,[102] and contributions from higher-lying MLCT states.

Emission Spectroscopy. The platinum compounds in this study are intensely luminescent in the solid-state at room temperature and in dilute solutions at 77 K. Figure 3 illustrates emission and excitation spectra of **1(a-d)** in glassy EMD solution at 77 K. Emission spectra of **2(a-b)** were obtained under similar conditions and are provided in Figure S5 (see ESI†). Table 2 summarizes emission data for these compounds.

Upon photoexcitation at λ 350 nm (and 400 nm), the low-temperature glassy solutions of **1(a-d)** give rise to one or more characteristic emission bands in 450-850 nm region. The first band beginning at in the range of λ_{max}(0-0) 540-560 nm is vibronically structured (1336-1450 cm^{-1} spacings), whereas the second band (maxima > 650 nm), absent from **1c**, is broad and structureless and displays a concentration dependence. The presence of any additional band(s) at longer wavelengths is discussed below. The emission of the $(PF_6)^-$ salt of **1a** is invariant from that of the Cl^- salt that we reported previously in frozen ethanol: methanol solution.[16] With reference to this Cl^- salt and related complexes,[16, 47, 88] the shortest wavelength vibronic emission of **1(a-d)**, excepting **1b**, is assigned to the $^3(\pi^*\rightarrow\pi)$ emission originating from the lowest spin-forbidden ^{3}LC (mbzimpy-centered) excited state (*Note*: The shortest wavelength emission of **1b**, we note (vide infra), originates from the significantly different excited state. Thus, to avoid confusion, hereinafter, whenever possible, we will discuss **1b** separately). Notably, energies and vibronic intensities of the ^{3}LC bands of **1(a, c, d)** are distinctly different from that of **3** (λ_{max} 462, 495, 530 nm; Huang-Rhys (HR) factor, (**S**) $I(1,0)/I(0,0)$ = 2.5)[47] and free mbzimpy (weak features at λ_{max} 457, 489, 520, 560, 608, S = 1.2) that exhibit emissions decidedly from the pure ^{3}LC states. Speaking of energies and vibronic intensities, the ^{3}LC bands of **1(a, c, d)** occur at relatively longer wavelengths than that of **3** and show smaller HR factors. For example, in the case of **1a,** the ^{3}LC band is red-shifted from that of the **3** by ~3500 cm^{-1} and displays **S** about 0.70. Seemingly, these changes are consistent with the notion that the ^{3}LC state of **1(a, c, d)** undergoes a perturbation upon interaction with the closely lying CT state.[47, 103, 104] Furthermore, the ^{3}LC band is bathochromically-shifted along the Cl < Ph < CH_3 series of ancillary ligands. Since, the corresponding ^{1}LC absorptions of **1(a, c, d)** occur at virtually identical energies, it is likely that the bathochromic-shift of ^{3}LC state along this order resulted in from its mixing with the higher-lying ^{3}MLCT state. This interpretation is in line with the absorption data (vide supra), which presents that the ^{1}MLCT state of **1(a, c, d)** is bathochromically-shifted along the Cl < Ph < CH_3 order as well.

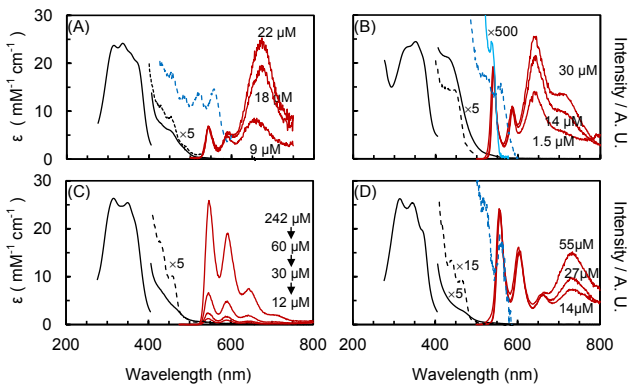

Figure 3. Room temperature electronic absorption spectrum in dimethyl sulfoxide (—), and 77 K emission (λ_{ex} = 400 nm, —) and excitation spectra (----, ----) in EMD glassy solution for A) **1a** (λ_{em} = 544 nm ---- ; λ_{em} = 670 nm , ----), B) **1b** (λ_{em} = 541 nm , ---- ; λ_{em} = 641 nm, —; λ_{em} = 709 nm , ----), C) **1c** (λ_{em} = 547 nm , ----), D) **1d** (λ_{em} = 557 nm , ---- ; λ_{em} = 735 nm, ----). Excepting for **1c**, the emission spectra at various concentrations are normalized at λ_{max} of the first vibronic feature. Absorption spectra in Figure 2 are duplicated in DMSO to facilitate visual comparison.

Surprisingly, the shortest wavelength emission band of **1b** (at λ_{max}, 541 nm) occurs at a relatively shorter wavelength than that of the **1(a, c, d)**. On energy grounds, the band is assigned to the ^{3}LLCT state. This assignment is consistent with the notion that the singlet-triplet (ΔE_{ST}) splitting is (generally) smaller for the CT states than that for the LC states; thus, the band will occur at relatively shorter wavelengths. The HR factor for this band, ~0.6 (Table 2), on the other hand, indicative of perturbation of ^{3}LLCT state, which is likely caused by the closely lying ^{3}MLCT state. These observations are congruous with the computational study (by TDDFT/CPCM) by Yam *et al.*,[95] that

suggests the lowest energy triplet emissive state of **1b** composed of transitions of ^{3}LLCT/^{3}MLCT mixed characters, and it originates from the HOMO (π-orbital of the phenyl acetylide ligand mixed with the platinum dπ-(d_{xz}/dyz) orbital) → LUMO (π*-orbital from mbzimpy) transitions.[95] Notably, the energy estimate for ^{3}LLCT/^{3}MLCT excited state (2.16 eV, ~ 573 nm) by TDDFT/CPCM (in CH_2Cl_2 at the optimized ground state)[95] is lower than 2.29 eV that we have estimated experimentally (in EMD). At this point, it is, however, unclear to what extent (consideration for) solvents will affect these estimates or this comparison for that matter.

Table 2. 77 K EtOH-MeOH-DMF [10:10:1 (v/v)] glassy solution emission data.

Compounds	λ_{max}, nm ($\lambda_{max\ Conc.\ dependent}$)	S (S^o)
1a	544, 590; 588, (655)	0.70 (0.54)
1b	541, 587, (641, 709)	0.59 (0.56)
1c	547, 592, 644, 709	0.70 (0.72)
1d	558, 604, 662, (734)	0.62 (0.63)
2a[a]	470, 506, 551, (578)	0.71
2b	534, 570, (695)	0.71
2c[a]	472, 507, 541, 581	1.20 (1.07)
2d[a]	471, 506, 542, (728)	0.68

[a]: 77K glassy butyronitrile solution

S: Huang-Rhys factor, *I*(1,0)/*I*(0,0).

S^o: Huang-Rhys factor, *I*(1,0)/*I*(0,0), obtained by deconvoluting the emission band into Gaussian components using Origin (OriginLab, Northampton, MA).

As noted above, **1(a, b, d)** also show a new band growing in with increasing concentration at longer wavelengths. The emission spectra of **1a** (Figure 3 (A)) show that the band at λ_{max} 655 nm (FWHM = ~1800 cm^{-1}) gains intensity relative to the higher energy emission features over the concentration range of 9-22 μM. The band further shows a bathochromic-shift of ~5 nm to 660 nm. As we noted earlier,[16] these observations are consistent with the formation of emissive aggregates, and the emission originates from the ^{3}MMLCT state. The excitation spectrum of **1a** monitored at λ_{em} 655 nm (Figure 3 (A)) exhibits a vibronically structured features at 556, 520, 485 nm (~1300 cm^{-1} spacings) which are attributable to ^{1}MMLCT [(dσ*(Pt)→π*(mbzimpy)] excited state.[16] Similarly, the emission bands at λ_{max} 641 and 734 nm in **1b** and **1d**, respectively, are attributable to the similar type of the aggregation-induced ^{3}MMLCT emissive state (Figure 3). Surprisingly, even though the emission maxima (for ^{3}MMLCT) varied distinctly in all three **1(a, b, d**), their corresponding excitation spectra display longer wavelength vibronic features at virtually identical energies (^{1}MMLCT at 556, 520 nm for **1b** and 558, 520 nm for **1d**). We also note that, in the case of **1d**, the emission from the aggregated species is weaker, and it is bathochromically-shifted by 1528 cm^{-1} from that of **1a**. The latter effect is consistent with the notion that the relatively stronger σ-donor methyl group enhances aggregation,[105] whereas the weaker emission is in accord with the energy-gap law which states that the rate of non-radiative decay increases exponentially with the decreasing excitation energy.[106-108] The emission spectra of **1b** also show a shoulder at 709 nm, which is gaining intensity with the concentration. The corresponding excitation spectrum monitored at this shoulder (λ_{em} 709 nm) shows a relatively weak absorption feature at 536 nm. Within the framework of plausible excited states and on energy grounds, this feature is attributable to ^{3}[π(-C≡CPh)→π*(mbzimpy)] state, and the emission likely originates from the aggregated species that is formed due mainly to ligand..ligand interactions.

Emissions of terpyridine **2(a-d)** complexes have previously been documented in various other rigid matrices[1, 4, 6, 29, 63, 65]. However, a dearth of the high-resolution spectral data in some cases had made it difficult for us to formulate as well as compare the electronic structural models. To counter this difficulty and to also maintain the uniformity in our measurements, very refined emission measurements have been carried out in EMD and butyronitrile matrices at 77 K (Figure S5 ESI†). Emission profiles of these complexes in both these matrices are nearly identical. As illustrated in Figure S5, like **1(a-d)**, the 77K butyronitrile glass of **2(a-d)** upon photoexcitation gave rise to one or more emission bands. Similarly, like **1b**, the emission of **2b** found emanating from the significantly different emitting state than that found in the rest of the tpy compounds, and it is thus presented here separately. The first and the shortest wavelength band of **2(a, c, d)** is vibronically structured (1200-1600 cm^{-1} spacings), which is diagnostic of ^{3}LC transitions. Surprisingly, the ^{3}LC band occurs at nearly identical wavelengths, λ_{max}(0-0) ~ 470 nm, in all three complexes. It should be noted that the corresponding parent ^{1}LC state (vide supra), however, is shifted somewhat to the longer wavelengths along the $CH_3 \approx Ph < Cl$ series. For example, $^1LC_1$ state of **2a** is red-shifted by ~ 900 cm^{-1} from that of the **2(c, d)**. The ^{3}LC emissions of **2(a, c, d)** also occur at longer wavelengths than that of the Zn(tpy)$^{2+}$ at 77K[109], which upon photoexcitation known to emit radiations from the pure ^{3}LC state. These observations, similar to that made earlier in the case **1**, are consistent with the notion that the shortest wavelength emissions of **2(a, c, d)** originate from the ^{3}(LC/MLCT) mixed states[4, 110] rather than from the pure LC states. At this point, it seems coincidental to have configuration mixing between ^{3}LC and ^{3}MLCT states being balanced in such a way that the shortest wavelength emitting states of **2(a, c, d)** occur at about the same energies. Provided that, the ^{3}(LC/MLCT) band of **2c** in contrast to that of the **2(a, d)** found displaying variation in the vibronic intensities, S = 1.2. But, on the other hand, to our surprise, the band also found displaying some similarities with that of the free terpyridine in frozen EMD glass[1], Zn(tpy)Cl_2 in dichloromethane at room-temperature[110] and Zn(4'-Ph-tpy)Cl_2 in ethylene glycol at 77K[111]. The emission from these latter species is assigned to the pure LC state. It is intriguing that despite the ^{3}LC state in all three **1(a, c, d)** has somewhat been perturbed by high-lying ^{3}MLCT state, the

emission profile (the shape and the vibronic intensities) of **2c** differs so significantly from that of the **2(a, d)**. While the source of this complexity is unclear, we believe it has likely resulted from the molecular distortion in the excited state. Given that the phenyl ring forms a dihedral angle of ~90° with the Pt coordination plane,[112-114] which in turn restricts a metal-tpy framework to only a minor distortion, we think, **2(a, d)** upon photoexcitation might be undergoing a considerable molecular distortion than that of **2c**.

In the case of **2b**, the shortest wavelength emission occurs at relatively low energy, λ_{max} = 534 nm (Figure S5 ESI†).[65] Although the band is poorly structured, it displays vibronic spacings of ~ 1200 cm^{-1} with S = 0.71, which is indicative of ligand involvement. Similar to **1b**, on energy grounds, this band is attributable to the ^{3}LLCT/^{3}MLCT mixed state. Consistent with this, the corresponding excitation spectrum measured at λ_{em} 534 nm displays dominating vibronic features at λ_{max} 430sh, 452 nm (1132 cm^{-1} spacing), that bear a mirror image relationship with the emission band above. These excitation features are assigned to metal perturbed ^{1}LLCT states. This assignment is congruous with the computational study by Yam *et al.*,[95] that suggests that the lowest energy excited/emitting states of **2b** arising from the admixture of LLCT/MLCT transitions. Notably, the energy estimate for these transitions (2.08 eV ≈ 596 nm) by TDDFT/CPCM (in CH_2Cl_2 at the optimized ground-state geometries)[95] is lower than the experimentally estimated value (< 534 nm). With that, we also note that, for **1b** and **2b**, the order of the relative energies for LLCT/MLCT transitions by experimental and computational calculations stand in contrast to each other (computationally, **1b** > **2b**; whereas experimentally **1b** < **2b**). On the other hand, ΔE_{ST} (experimental) for LLCT/MLCT state is 3988 cm^{-1} for **1b** and 3397 cm^{-1} for **2b**, which is consistent with the notion that MLCT character is relatively higher in **2b**.

Like mbzimpy analogs, the **2(a-d)** complexes, excepting **2c**, display a broad and structureless emission in the 550-800 nm region due to the formation of emissive aggregates. These features are attributable to the ^{3}MMLCT [(dσ*(Pt) → π*(tpy)] transitions, and display a red-shift along Cl < CCPh < CH_3 series of ancillary ligand which is indicative of enhancement of platinum-platinum interaction along the same order due mainly to an increased σ-donor capacity of ancillary ligand. The excitation spectra monitored at the λ_{max} of these ^{3}MMLCT emissive features reveal weak absorption features at 411, 439, 471 nm for **2a**, and 458, 490sh nm (1426 cm^{-1} spacings) for **2b**, and 440, 466 and 496 nm for **2d**. On energy grounds, we tentatively assign these features to ^{1}MMLCT transitions.

Electronic Structure: Mixing between ^{3}LC and ^{3}MLCT States.

Based on the spectroscopic data described above, an energy-level diagram can be drawn. The diagram in figure 4 gives a qualitative and quantitative overview of various low lying excited and emitting states of **1** and **2**. The energy values shown are absolute values with respect to the ground state. The mixed states in the diagram are labelled only with the main character of the state. It is conspicuous from the diagram that the excited states of mbzimpy and tpy complexes with similar orbital parentage differ distinctly in energies. Furthermore, a given an excited state of **1** and **2** has been influenced/perturbed quite differently by the same group of ancillary ligands. This behavior could principally be resulted from a) energies of the frontier orbitals of **1** being at different levels from that of **2**, which brings b) variations in the extent of configuration mixing between the frontier molecular orbitals, and hence between LC and MLCT states. Since the orbital parentage of the lowest-energy excited state of phenylacetylene adducts (**1b, 2b)** differ significantly from the rest of the compounds, to avoid ambiguity, these compounds have been divided into two subgroups. Below, **1(a, c, d)** and **2(a, c, d)** are briefly mentioned as a group A complexes and **1b, 2b** as a group B complexes.

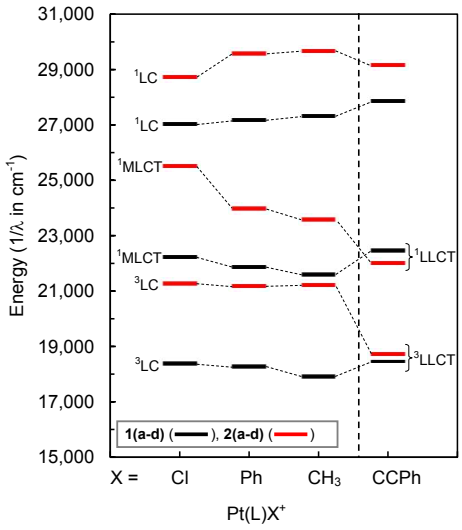

Figure 4. State energy level diagram for Pt(mbzimpy)X^+ (in black) and Pt(tpy)X^+ (in Red) complexes. Energies were derived from spectroscopic data. Some mixed excited and emissive states are labelled only with the main character (for details, see the text).

As can be seen from the diagram, the lowest energy ^{1}LC excited states of group A compounds are destabilized along the Cl < Ph < CH_3 series of ancillary ligands. In the case of mbzimpy compounds, the ^{1}LC state energies, however, seem to be unaltered (or less affected), although the electrochemistry of both **1** and **2** indicates a perturbation of LUMO-π* by somewhat identical energies. This unusual behavior implies that a perturbation also likely occurs in the donor π-MOs in a similar fashion, which leaves the energy of ^{1}LC state somewhat unaffected along the Cl < Ph < CH_3 series. Whereas, in the case of terpyridyl compounds, the donor π-MOs are presumably

weakly perturbed. On the other hand, both analogs display stabilization of the ^{1}MLCT state along the Cl < Ph < CH_3 series.

In contrast to the ^{1}LC state, the ^{3}LC emitting state of mbzimpy compounds is stabilized along the Cl < Ph < CH_3 series with ΔE_{ST} (single–triplet splitting energy) increasing linearly from 8645 cm^{-1} to 9400 cm^{-1}. Although, energies of the ^{3}LC emitting states of terpyridyl compounds do not appear to be sensitive to the σ-donation of ancillary ligands, the ΔE_{ST} found linearly increasing from 7450 cm^{-1} to 8440 cm^{-1} along the Cl < Ph < CH_3 series as well. We believe that the stabilization of the ^{3}LC state along these series likely resulted from its mixing with the higher lying ^{3}MLCT state. Furthermore, it is conspicuous from the diagram that the energy gap between ^{3}LC and ^{1}MLCT states is narrowing along the Cl < Ph < CH_3 order. Thus, the coupling between ^{3}MLCT and ^{3}LC states is expected to increase in the same order.

Interestingly, in the case of group B complexes, the low-lying ^{1}(LLCT/MLCT) excited states occur at approximately the same energies. In the case of **1b**, the energy of this state, however, is approximate because of not having a well-defined emission-excitation spectrum. Notably, the ^{3}(LLCT/MLCT) emitting states of **1b** and **2b** also occur at approximately the same energies with ΔE_{ST} being ~ 3988 cm^{-1} for **1b** and ~ 3300 cm^{-1} for **2b**. A relatively low ΔE_{ST} value for **2b** indicates higher MLCT character in ^{3}(LLCT/MLCT) emitting state, which we believe is the underlying cause for emission of **2b** being relatively weakly structured.

On the other hand, the energies of the MMLCT states of **1** and **2** are consistent with the notion that the mbzimpy compounds undergo relatively stronger Pt..Pt interactions, leading the formation of aggregates, presumably dimers. Furthermore, the energies of the ^{3}MMLCT states of methyl adducts (**1d**, **2d**) are found at relatively low energy level within the series, which indicates that these compounds undergo much stronger metal..metal interactions.

Conflicts of interest

There are no conflicts to declare.

Acknowledgments

We thank the NSF (Grants CHE-1152853 & CHE-1566438); and the Department of Chemistry, University of Cincinnati (UC), for NMR and Mass Spectrometry facilities. V.M.S. thanks Drs. S. Macha and L. Sallans (UC) for expert technical assistance with mass spectrometry, and Drs. K. Ding and N. Kaval (UC) for assistance with NMR and FTIR, respectively. V.M.S also thanks Dr. J. A. Krause (Crystallographer at UC) for confirming the structural identities of **1b** and **1c** by single X-ray crystallography.

Notes and references

1. J. A. Bailey, M. G. Hill, R. E. Marsh, V. M. Miskowski, W. P. Schaefer and H. B. Gray, *Inorg. Chem.*, 1995, **34**, 4591-4599.
2. M. G. Hill, J. A. Bailey, V. M. Miskowski and H. B. Gray, *Inorg. Chem.*, 1996, **35**, 4585-4590.
3. T. K. Aldridge, E. M. Stacy and D. R. McMillin, *Inorg. Chem.*, 1994, **33**, 722-727.
4. G. Arena, G. Calogero, S. Campagna, L. M. Scolaro, V. Ricevuto and R. Romeo, *Inorg. Chem.*, 1998, **37**, 2763-2769.
5. K. W. Jennette, J. T. Gill, J. A. Sadownick and S. J. Lippard, *J. Am. Chem. Soc.*, 1976, **98**, 6159-6168.
6. H. K. Yip, L. K. Cheng, K. K. Cheung and C. M. Che, *J. Chem. Soc., Dalton Trans.*, 1993, 2933-2938.
7. W.-S. Tang, X.-X. Lu, K. M.-C. Wong and V. W.-W. Yam, *J. Mater. Chem.*, 2005, **15**, 2714-2720.
8. M. L. Muro, C. A. Daws and F. N. Castellano, *Chem. Commun.*, 2008, 6134-6136.
9. S. D. Taylor, W. Howard, N. Kaval, R. Hart, J. A. Krause and W. B. Connick, *Chem. Commun.*, 2010, **46**, 1070-1072.
10. S. Chatterjee, A. E. Norton, M. K. Edwards, J. M. Peterson, S. D. Taylor, S. A. Bryan, A. Andersen, N. Govind, T. E. Albrecht-Schmitt, W. B. Connick and T. G. Levitskaia, *Inorg. Chem.*, 2015, **54**, 9914-9923.
11. P. Du, J. Schneider, P. Jarosz, J. Zhang, W. W. Brennessel and R. Eisenberg, *J. Phys. Chem. B*, 2007, **111**, 6887-6894.
12. T. J. Wadas, Q.-M. Wang, Y.-J. Kim, C. Flaschenreim, T. N. Blanton and R. Eisenberg, *J. Am. Chem. Soc.*, 2004, **126**, 16841-16849.
13. Y. Yang, D. Zhang, L.-Z. Wu, B. Chen, L.-P. Zhang and C.-H. Tung, *J. Org. Chem.*, 2004, **69**, 4788-4791.
14. M. Cortes, J. T. Carney, J. D. Oppenheimer, K. E. Downey and S. D. Cummings, *Inorg. Chim. Acta*, 2002, **333**, 148-151.
15. P. Du, J. Schneider, P. Jarosz and R. Eisenberg, *J. Am. Chem. Soc.*, 2006, **128**, 7726-7727.
16. L. J. Grove, J. M. Rennekamp, H. Jude and W. B. Connick, *J. Am. Chem. Soc.*, 2004, **126**, 1594-1595.
17. J. R. Kumpfer, S. D. Taylor, W. B. Connick and S. J. Rowan, *J. Mater. Chem.*, 2012, **22**, 14196-14204.
18. A. Y.-Y. Tam, W. H. Lam, K. M.-C. Wong, N. Zhu and V. W.-W. Yam, *Chem. - Eur. J.*, 2008, **14**, 4562-4576.
19. A. Y.-Y. Tam, K. M.-C. Wong and V. W.-W. Yam, *J. Am. Chem. Soc.*, 2009, **131**, 6253-6260.
20. I. Mathew and W. Sun, *Dalton Trans.*, 2010, **39**, 5885-5898.
21. N. Liu, B. Wang, W. Liu and W. Bu, *Chem. Commun.*, 2011, **47**, 9336-9338.
22. B. Jiang, J. Zhang, J.-Q. Ma, W. Zheng, L.-J. Chen, B. Sun, C. Li, B.-W. Hu, H. Tan, X. Li and H.-B. Yang, *J. Am. Chem. Soc.*, 2016, **138**, 738-741.
23. K. Zhang, M. C.-L. Yeung, S. Y.-L. Leung and V. W.-W. Yam, *Chem*, 2017, **2**, 825-839.
24. K. Wang, M.-a. Haga, H. Monjushiro, M. Akiba and Y. Sasaki, *Inorg. Chem.*, 2000, **39**, 4022-4028.
25. I. Eryazici, C. N. Moorefield and G. R. Newkome, *Chem. Rev.*, 2008, **108**, 1834-1895.
26. M.-C. Tang, A. K.-W. Chan, M.-Y. Chan and V. W.-W. Yam, *Top. Curr. Chem.*, 2016, **374**, 46.
27. K. M.-C. Wong and V. W.-W. Yam, *Coord. Chem. Rev.*, 2007, **251**, 2477-2488.

28. O. S. Wenger, *Chem. Rev.*, 2013, **113**, 3686-3733.
29. D. R. McMillin and J. J. Moore, *Coord. Chem. Rev.*, 2002, **229**, 113-121.
30. P. Wang, C.-H. Leung, D.-L. Ma, S.-C. Yan and C.-M. Che, *Chem.: Eur. J.*, 2010, **16**, 6900-6911.
31. V. M. Shingade, Ph.D. Dissertation, University of Cincinnati, 2016.
32. V. C.-H. Wong, C. Po, S. Y.-L. Leung, A. K.-W. Chan, S. Yang, B. Zhu, X. Cui and V. W.-W. Yam, *J. Am. Chem. Soc.*, 2018, **140**, 657-666.
33. C. E. Buss, C. E. Anderson, M. K. Pomije, C. M. Lutz, D. Britton and K. R. Mann, *J. Am. Chem. Soc.*, 1998, **120**, 7783-7790.
34. C. E. Buss and K. R. Mann, *J. Am. Chem. Soc.*, 2002, **124**, 1031-1039.
35. S. M. Drew, D. E. Janzen, C. E. Buss, D. I. MacEwan, K. M. Dublin and K. R. Mann, *J. Am. Chem. Soc.*, 2001, **123**, 8414-8415.
36. E. J. Rivera, C. Barbosa, R. Torres, L. Grove, S. Taylor, W. B. Connick, A. Clearfield and J. L. Colon, *J. Mater. Chem.*, 2011, **21**, 15899-15902.
37. L. J. Grove, A. G. Oliver, J. A. Krause and W. B. Connick, *Inorg. Chem.*, 2008, **47**, 1408-1410.
38. S. D. Taylor, Ph.D. Dissertation, University of Cincinnati, 2011.
39. L. J. Grove, Ph.D. Dissertation, University of Cincinnati, 2007.
40. H. K. Yip, L. K. Cheng, K. K. Cheung and C. M. Che, *J.Chem. Soc., Dalton Trans.*, 1993, 2933-2938.
41. D. K. Crites, C. T. Cunningham and D. R. McMillin, *Inorg. Chim. Acta*, 1998, **273**, 346-353.
42. R. Buechner, J. S. Field, R. J. Haines, C. T. Cunningham and D. R. McMillin, *Inorg. Chem.*, 1997, **36**, 3952-3956.
43. G. Guglielmo, V. Ricevuto, A. Giannetto and S. Campagna, *Gazz. Chim. Ital.*, 1989, **119**, 457-460.
44. G. Arena, G. Calogero, S. Campagna, L. M. Scolaro, V. Ricevuto and R. Romeo, *Inorg. Chem.*, 1998, **37**, 2763-2769.
45. J. A. Bailey, M. G. Hill, R. E. Marsh, V. M. Miskowski, W. P. Schaefer and H. B. Gray, *Inorg. Chem.*, 1995, **34**, 4591-4599.
46. G. W. Gokel, Dean's Handbook of Organic Chemistry, 2nd ed., 2004.
47. T. Yutaka, S. Obara, S. Ogawa, K. Nozaki, N. Ikeda, T. Ohno, Y. Ishii, K. Sakai and M.-a. Haga, *Inorg. Chem.*, 2005, **44**, 4737-4746.
48. V. Shklover, I. L. Eremenko, H. Berke, R. Nesper, S. M. Zakeeruddin, M. K. Nazeeruddin and M. Grätzel, *Inorg. Chim. Acta*, 1994, **219**, 11-21.
49. S. B. Sanni, H. J. Behm, P. T. Beurskens, A. G. A. Van, J. Reedijk, A. T. H. Lenstra, A. W. Addison and M. Palaniandavar, *J. Chem. Soc., Dalton Trans.*, 1988, 1429-1435.
50. X. Wang, S. Wang, L. Li, E. B. Sundberg and G. P. Gacho, *Inorg. Chem.*, 2003, **42**, 7799-7808.
51. S. A. Cotton, V. Franckevicius and J. Fawcett, *Polyhedron*, 2002, **21**, 2055-2061.
52. G. Francese, H. W. Schmalle and S. Decurtins, *Acta Crystallogr. C*, 1999, **55**, 730-733.
53. H. Oshio, H. Spiering, V. Ksenofontov, F. Renz and P. Gütlich, *Inorg. Chem.*, 2001, **40**, 1143-1150.
54. B. Figgis, E. Kucharski and A. White, *Aust. J. Chem.*, 1983, **36**, 1527-1535.
55. F. Takusagawa, P. G. Yohannes and K. B. Mertes, *Inorg. Chim. Acta*, 1986, **114**, 165-169.
56. J.-P. Collin, I. M. Dixon, J.-P. Sauvage, J. A. G. Williams, F. Barigelletti and L. Flamigni, *J. Am. Chem. Soc.*, 1999, **121**, 5009-5016.
57. W.-W. Yang, Y.-W. Zhong, S. Yoshikawa, J.-Y. Shao, S. Masaoka, K. Sakai, J. Yao and M.-a. Haga, *Inorg. Chem.*, 2012, **51**, 890-899.
58. X. Xiao, M. Haga, T. Matsumura-Inoue, R. Yu, A. W. Addison and K. Kano, *J. Chem. Soc., Dalton Trans.*, 1993, 2477-2484.
59. S. Flores-Torres, G. R. Hutchison, L. J. Soltzberg and H. D. Abruna, *J. Am. Chem. Soc.*, 2006, **128**, 1513-1522.
60. C. R. Arana and H. D. Abruna, *Inorg. Chem.*, 1993, **32**, 194-203.
61. G. Annibale, M. Brandolisio and B. Pitteri, *Polyhedron*, 1995, **14**, 451-453.
62. M. Howe-Grant, S. J. Lippard, P. Chalilpoyil and L. G. Marzilli, in *Inorg. Synth.*, 2007, 101-105.
63. Q.-Z. Yang, L.-Z. Wu, Z.-X. Wu, L.-P. Zhang and C.-H. Tung, *Inorg. Chem.*, 2002, **41**, 5653-5655.
64. G. S. Hill, M. J. Irwin, C. J. Levy, L. M. Rendina and R. J. Puddephatt, *Inorg. Synth.*, 1998, **32**, 149-153.
65. V. W.-W. Yam, R. P.-L. Tang, K. M.-C. Wong and K.-K. Cheung, *Organometallics*, 2001, **20**, 4476-4482.
66. P. T. Kissinger and W. R. Heineman, *J. Chem. Educ.*, 1983, **60**, 702-706.
67. A. W. Addison, S. Burman, C. G. Wahlgren, O. A. Rajan, T. M. Rowe and E. Sinn, *J. Chem. Soc., Dalton Trans.*, 1987, 2621-2630.
68. C. Piguet, G. Bernardinelli and A. F. Williams, *Inorg. Chem.*, 1989, **28**, 2920-2925.
69. A. F.-F. Cheung, E. Y.-H. Hong and V. W.-W. Yam, *Chem. - Eur. J.*, 2018, **24**, 1383-1393.
70. C. Po, A. Y.-Y. Tam, K. M.-C. Wong and V. W.-W. Yam, *J. Am. Chem. Soc.*, 2011, **133**, 12136-12143.
71. G. Jones and V. I. Vullev, *J. Phys. Chem. A*, 2001, **105**, 6402-6406.
72. J. D. Crowley and B. Bosnich, *Eur. J. Inorg. Chem.*, 2005, **2005**, 2015-2025.
73. A. Gourdon and J.-P. Launay, *Inorg. Chem.*, 1998, **37**, 5336-5341.
74. X. Wang, Y. Shen, Y. Pan and Y. Liang, *Langmuir*, 2001, **17**, 3162-3167.
75. S. H. Toma, M. Uemi, S. Nikolaou, D. M. Tomazela, M. N. Eberlin and H. E. Toma, *Inorg. Chem.*, 2004, **43**, 3521-3527.
76. M. Franco, K. Araki, R. Rocha and H. Toma, *J. Solution Chem.*, 2000, **29**, 667-684.
77. V. M. Shingade, W. B. Connick, Manuscript in Preparation.
78. J. C. Evans and R. A. Nyquist, *Spectrochim. Acta*, 1960, **16**, 918-928.
79. R. A. Nyquist and S. Fiedler, *Vib. Spectrosc.*, 1994, **7**, 149-162.
80. A. S. Goldman and K. Krogh-Jespersen, *J. Am. Chem. Soc.*, 1996, **118**, 12159-12166.

81. V. W.-W. Yam, K. H.-Y. Chan, K. M.-C. Wong and N. Zhu, *Chem.: Eur. J.*, 2005, **11**, 4535-4543.
82. K. M.-C. Wong, W.-S. Tang, B. W.-K. Chu, N. Zhu and V. W.-W. Yam, *Organometallics*, 2004, **23**, 3459-3465.
83. S. Chakraborty, T. J. Wadas, H. Hester, R. Schmehl and R. Eisenberg, *Inorg. Chem.*, 2005, **44**, 6865-6878.
84. X. Liu, E. J. L. McInnes, C. A. Kilner, M. Thornton-Pett and M. A. Halcrow, *Polyhedron*, 2001, **20**, 2889-2900.
85. L. Yang, F. L. Wimmer, S. Wimmer, J. Zhao and P. S. Braterman, *J. Organomet. Chem.*, 1996, **525**, 1-8.
86. T. Yutaka, I. Mori, M. Kurihara, J. Mizutani, N. Tamai, T. Kawai, M. Irie and H. Nishihara, *Inorg. Chem.*, 2002, **41**, 7143-7150.
87. N. Elgrishi, M. B. Chambers, V. Artero and M. Fontecave, *Phys. Chem. Chem. Phys.*, 2014, **16**, 13635-13644.
88. S. Ruettimann, C. M. Moreau, A. F. Williams, G. Bernardinelli and A. W. Addison, *Polyhedron*, 1992, **11**, 635-646.
89. We note that $[Zn(mbzimpy)_2](PF_6)_2$ complex in 0.1 M TBAH/DMF exhibits quasi-reversible ligand-based reductions at -1.13 and -1.33 volts vs. Ag/AgCl (3 M NaCl). These potentials are comparable with the electrochemical data for the same in prolylene carbonate (-1.05 and -1.23 volts vs. NHE) reported by Addison et al. (Polyhedron 1992, 11, 635).
90. C. B. Blanton, Z. Murtaza, R. J. Shaver and D. P. Rillema, *Inorg. Chem.*, 1992, **31**, 3230-3235.
91. P. Jarosz, J. Thall, J. Schneider, D. Kumaresan, R. Schmehl and R. Eisenberg, *Energy Environ. Sci.*, 2008, **1**, 573-583.
92. S. Chakraborty, T. J. Wadas, H. Hester, C. Flaschenreim, R. Schmehl and R. Eisenberg, *Inorg. Chem.*, 2005, **44**, 6284-6293.
93. E. Shikhova, E. O. Danilov, S. Kinayyigit, I. E. Pomestchenko, A. D. Tregubov, F. Camerel, P. Retailleau, R. Ziessel and F. N. Castellano, *Inorg. Chem.*, 2007, **46**, 3038-3048.
94. Q.-Z. Yang, Q.-X. Tong, L.-Z. Wu, Z.-X. Wu, L.-P. Zhang and C.-H. Tung, *Eur. J. Inorg. Chem.*, 2004, DOI: 10.1002/ejic.200300878, 1948-1954.
95. W. H. Lam, E. S.-H. Lam and V. W.-W. Yam, *J. Am. Chem. Soc.*, 2013, **135**, 15135-15143.
96. K. Nakamoto, *J. Phys. Chem.*, 1960, **64**, 1420-1425.
97. D. W. Fink and W. E. Ohnesorge, *J. Phys. Chem.*, 1970, **74**, 72-77.
98. D. P. Lazzaro, P. E. Fanwick and D. R. McMillin, *Inorg. Chem.*, 2012, **51**, 10474-10476.
99. W. F. Fleeman and W. B. Connick, *Comments Inorg. Chem.*, 2002, **23**, 205-230.
100. W. B. Connick, V. M. Miskowski, V. H. Houlding and H. B. Gray, *Inorg. Chem.*, 2000, **39**, 2585-2592.
101. M. L. Myrick and M. K. De Armond, *J. Phys. Chem.*, 1989, **93**, 7099-7107.
102. M. G. Hill, J. A. Bailey, V. M. Miskowski and H. B. Gray, *Inorg. Chem.*, 1996, **35**, 4585-4590.
103. V. M. Miskowski and V. H. Houlding, *Inorg. Chem.*, 1991, **30**, 4446-4452.
104. W. B. Connick, V. M. Miskowski, V. H. Houlding and H. B. Gray, *Inorg. Chem.*, 2000, **39**, 2585-2592.
105. V. M. Shingade, W. B. Connick, Manuscript in Preparation.
106. R. Englman and J. Jortner, *Mol. Phys.*, 1970, **18**, 145-164.
107. J. S. Wilson, N. Chawdhury, M. R. Al-Mandhary, M. Younus, M. S. Khan, P. R. Raithby, A. Kohler and R. H. Friend, *J. Am. Chem. Soc.*, 2001, **123**, 9412-9417.
108. M. Bixon and J. Jortner, *J. Chem. Phys.*, 1968, **48**, 715-726.
109. T. Ohno, S. Kato, S. Kaizaki and I. Hanazaki, *Inorg. Chem.*, 1986, **25**, 3853-3858.
110. J. F. Michalec, S. A. Bejune, D. G. Cuttell, G. C. Summerton, J. A. Gertenbach, J. S. Field, R. J. Haines and D. R. McMillin, *Inorg. Chem.*, 2001, **40**, 2193-2200.
111. J. J. Moore, J. J. Nash, P. E. Fanwick and D. R. McMillin, *Inorg. Chem.*, 2002, **41**, 6387-6396.
112. S. B. Harkins and J. C. Peters, *Organometallics*, 2002, **21**, 1753-1755.
113. H. Jude, J. A. K. Bauer and W. B. Connick, *J. Am. Chem. Soc.*, 2003, **125**, 3446-3447.
114. D. Zhao, J. A. Krause and W. B. Connick, *Inorg. Chem.*, 2015, **54**, 8339-8347.

For Table of Contents Entry Only

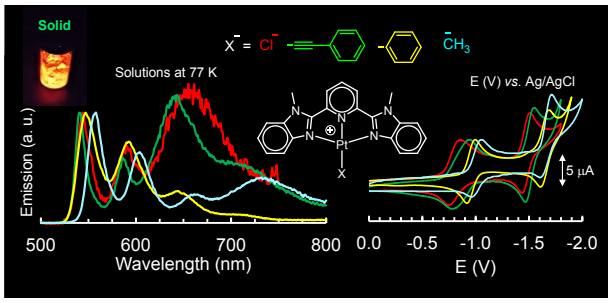

Spectroscopic and electrochemical properties of highly luminescent Pt(2,6-bis(*N*-methylbenzimidazol-2-yl)pyridine)X^+ have been discussed and contrasted with the archetypal Pt(2,2';6',2"-terpyridine)X^+ for better understanding of their electronic structures.